JOURNAL OF MATERIALS SCIENCE **39** (2004) 975–985

Study on high-temperature naphthenic acid corrosion and erosion-corrosion of aluminized carbon steel

X. Q. WU*, H. M. JING, Y. G. ZHENG, Z. M. YAO, W. KE
State Key Laboratory for Corrosion and Protection, Institute of Metal Research, South Campus, Chinese Academy of Sciences, 62 Wencui Road, Shenyang 110016, People's Republic of China
E-mail: wxq_imr@yahoo.com

High-temperature naphthenic acid corrosion (NAC) and erosion-corrosion (NAEC) behaviors of pack-aluminized carbon steel have been investigated in laboratory to evaluate the resistance of aluminized layer to the NAC and NAEC. A field erosion-corrosion test of 700 days was also performed in an oil refinery. Parallel tests were carried out for carbon steel. It was found that the aluminized steel exhibited a better NAC resistance only at early testing stage than the carbon steel in high total-acid-number (TAN) environment. The NAC resistance degraded rapidly with increasing testing time, and became even worse than that of the carbon steel at final testing stage, accompanying a step-like or lamellar spallation in the aluminized layer. In low TAN environment, the aluminized steel exhibited a much better resistance to both the NAC and NAEC in comparison with the carbon steel. Similarly a good erosion-corrosion resistance was found for the aluminized steel in actual oil-refining environment although relatively serious erosion-corrosion attack simultaneously took place in the aluminized layer. Based on the above results, possible NAC and NAEC mechanisms for the aluminized steel are discussed.

1. Introduction

High temperature crude corrosivity of distillation units in oil refineries, especially caused by naphthenic acids and sulfur compounds, is a major concern to the oil-refining industry worldwide. In recent years, an increased interest has been focused on naphthenic acid corrosion (NAC) in oil refineries due to gradually increased exploitation and refining of acidic crude oils from many parts of the word such as China, India, Venezuela, Eastern Europe, Russia and USA [1]. The potential component failures owing to the NAC have become a critical safety and reliability issue in oil refineries, especially at the locations where the fluid velocity is relatively fast or the acid concentration is relatively high. Typically susceptible locations or components are the transfer lines, furnace tubes, valves, baffles, pumps, fittings, feed and reflux sections of columns, trays, walls of columns, and so on. Developing NAC-resistant materials or improving NAC resistance of the materials used for present oil-refining installations, thus, become quite necessary and urgent.

Although damage due to the NAC in oil refineries has been found for about eighty years [2], the nature of this corrosion process and its controlling factors keep still ambiguous due to the complex influencing factors of NAC and a deficiency in systematical experimental study on this aspect. Most of existing technical documents on NAC primarily deal with case histories [1–19]. At present, four paths are usually employed to diminish or resist the NAC in oil refineries, including (i) improving the oil-refining process, such as blending, injection of inhibitors, de-acidification of crude oils, reducing the activity of organic acids in crude oils, and so on. (ii) improving the fluid velocity and the flow pattern, mainly by optimizing the structure design of the oil-refining installations or components. (iii) improving the corrosion resistance of components materials, such as material upgrading, surface modification (coatings or lining), and so on. (iv) developing or improving the techniques of in-service monitoring. According to field surveys, the third path is the most common and effective measurement to resist the NAC in actual oil-refining environment currently [10].

So far the aluminizing processes have been extensively and successfully used in high temperature corrosion prevention of oil-refining components, especially in the aspect of resisting sulfur compound corrosion. However, systematically experimental work associated with the influence of aluminizing treatments on the NAC resistance of components materials in oil-refineries is still deficient relatively. In the present study, the NAC and naphthenic acid erosion-corrosion

*Author to whom all correspondence should be addressed.

(NAEC) behaviors of pack-aluminized carbon steel have been investigated in laboratory. A field erosion-corrosion test of 700 days in an oil refinery was performed to evaluate the NAC and NAEC resistance of the aluminized layer. Parallel tests were also carried out for carbon steel for comparison purpose.

2. Experimental

2.1. Experimental materials and specimens

The material used in present study was hot-rolled carbon steel plate, whose chemical compositions (wt%) are 0.16C, 0.20Si, 0.45Mn, 0.30Cu, <0.04P, <0.04S, and Fe balanced. The microstructure consisted of ferrite and pearlite and the microhardness was about 150. Disc specimens with diameter of 16 mm were machined from the hot-rolled plate and were used in laboratory tests, while rectangle specimens with size of 70 × 30 mm were used in field test. The aluminized specimens were prepared by a pack-aluminizing method. The aluminizing agents consisted of aluminum powder, iron-aluminum alloy powder, and activators. The aluminizing temperature and time were 900°C and 4 h respectively. Fig. 1 shows the surface and cross-section morphology of the aluminized specimens. X-ray diffraction analysis revealed that the aluminized layer was mainly composed of $Fe_{0.5}Al_{0.5}$ phase (Fig. 1c). The thickness of the aluminized layer was about 160 μm and its highest microhardness was 530 (Fig. 1d).

2.2. Experimental parameters and procedures

The NAC tests were performed by an immersion method in an autoclave, while NAEC tests were carried out using a set of hot oil loop as stated in previous study [20]. The media for the NAC and NAEC tests in laboratory were a mixture of transformer-oil and refining naphthenic acids. The total acid number (TAN) of the media was adjusted by changing the mixture ratio and was measured by a titration method [7]. The field erosion-corrosion test was performed in an oil refinery. The testing duration was 700 days. The test specimens were fixed by two bolts on the support poles of the feeding entry of atmosphere column, which was one of the most serious erosion-corrosion locations in this oil refinery. The specimens' surfaces were vertical to the direction of the jet impingement center of the feeding fluid. The medium was the bottom oil of primary distillation tower and the correspondingly environmental parameters are shown in Table I.

Before and after tests, the specimens were ultrasonically degreased and rinsed by acetone, dried in air and weighed. The NAC or NAEC rate U with units of mm/yr was calculated as follows

$$U = \frac{\Delta w}{\rho S t} \times 24 \times 365 \tag{1}$$

here ρ is the material density with units of g/mm^3, S is the corrosion or erosion-corrosion area with units

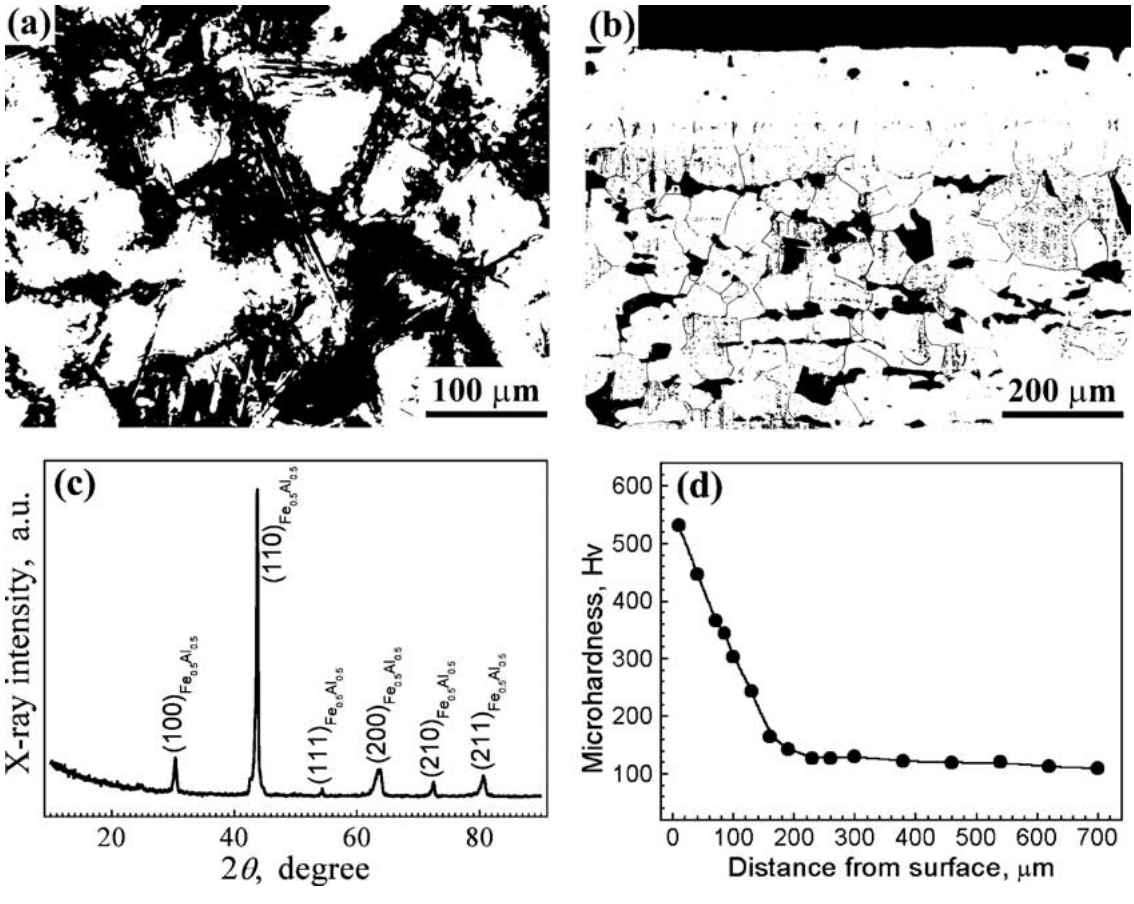

Figure 1 (a) Surface morphology and (b) cross-section morphology of the aluminized carbon steel. (c) X-ray analysis and (d) microhardness of the aluminized layer.

TABLE I Environmental parameters of the field test of 700 days in an oil refinery

Testing location	Temperature (°C)	Pressure (atm)	TAN (mgKOH/g)	Sulfur content (%)
Feeding entry of the atmosphere column	360–365	1.0	0.9–1.2	0.8–1.0

of mm^2, t is the corrosion or erosion-corrosion time with units of h, and Δw is the weight loss of samples caused by NAC or NAEC with units of g. An optical microscope and a JSM-6301F scanning electron microscopy (SEM) with an ISIS300 Series energy-dispersive X-ray analyzer (EDX) were used for morphology observation and composition analyses.

3. Results

3.1. NAC tests in laboratory

Fig. 2 shows dependence of the immersion duration on the NAC rate at 250°C in high-TAN (210 mgKOH/g) environment. For the carbon steel, the NAC rate increased rapidly at the early stage of immersion, remained comparatively constant from 30 to 100 h, and after then, decreased slightly. For the aluminized steel, a distinct incubation-like period with low NAC rate, which was about one order of magnitude lower than that of the carbon steel, appeared at the early stage of immersion. Then, the NAC rate increased rapidly from 10 to 100 h and afterwards decreased gradually. Clearly, in high-TAN environment, the aluminized steel exhibited a much better resistance to the NAC than the carbon steel only at the early stage of immersion. The NAC resistance of the aluminized steel degraded rapidly with increasing immersion time, and became even worse than that of the carbon steel at the final stage of immersion. Fig. 3 shows dependence of the experimental temperatures on the NAC rate in high-TAN environment. Increased the temperatures markedly increased the NAC rate for both the carbon steel and the aluminized steel, especially in high-temperature region. After 100 h immersion at all temperatures, the aluminized steel showed a worse NAC resistance compared to the carbon steel.

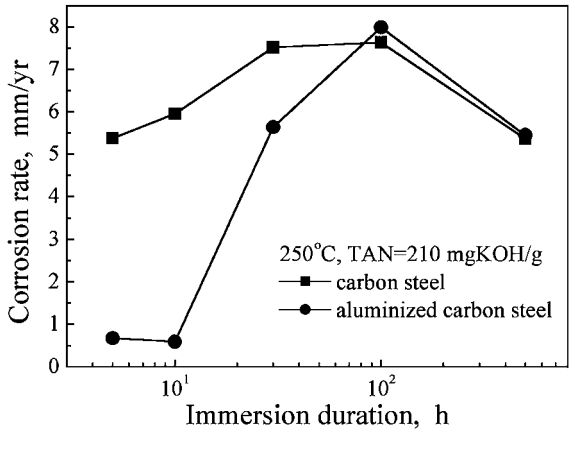

Figure 2 Dependence of NAC rate on the immersion duration.

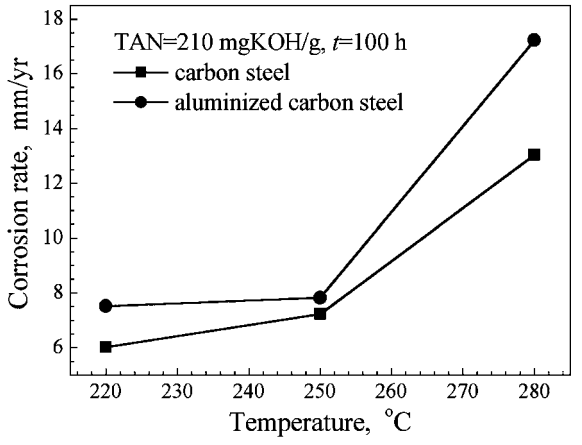

Figure 3 Dependence of NAC rate on the experimental temperature.

Fig. 4 shows development of NAC morphology of the aluminized steel in high-TAN environment with increasing immersion duration. At the early stage of immersion, the NAC predominantly took place at grain boundaries. Corrosion pits also appeared on some grain surfaces (Fig. 4a). Increasing the immersion time remarkably aggravated the pitting (Fig. 4b). At this stage, the aluminized layer still kept integrated and adhered to the matrix, coinciding with the low NAC rate as shown in Fig. 2. Further increasing the immersion time, serious spallation took place in the aluminized layer, accompanying the onset of corrosion of the substrate (Fig. 4c), which was in correspondence with rapid increase in NAE rate. After 500 h immersion, the aluminized layer scaled off completely (Fig. 4d). EDX analysis revealed that the substrate, i.e., the carbon steel, had been corroded severely (Fig. 5).

Fig. 6 shows typical NAC morphology after 100 h immersion at 220°C. The carbon steel suffered from inhomogenous NAC. The grain boundaries and some corrosion-susceptible grains were severely corroded (Fig. 6a). However, relatively homogenous NAC took place on the surface of the aluminized steel (Fig. 6b). EDX analysis revealed that the surface was still rich in aluminum relatively (Fig. 7), which suggested that the aluminized layer had not failed completely despite suffering from severe attack. Observed at high magnification, it was found that the aluminized layer degraded in a step-like (Fig. 6c) or laminar spallation (Fig. 6d), which was very similar to the rock-candy patterns of brittle fracture. There existed distinct boundaries between the two steps with different orientation. Some of boundaries consisted of metal remnants whose morphology was very similar to the intergranular precipitation (Fig. 6e), while the others were cracks, as indicated by arrows in Figs 6c and d. Table II shows the

TABLE II EDX analysis of the aluminized steel after 100 h immersion in high-TAN environment at 220°C (wt%)

Areas	Al	Fe	S	Ni
A	10.35	86.84	0.77	2.04
B	5.88	93.20	0.45	0.47
C	16.84	78.84	0.99	3.33

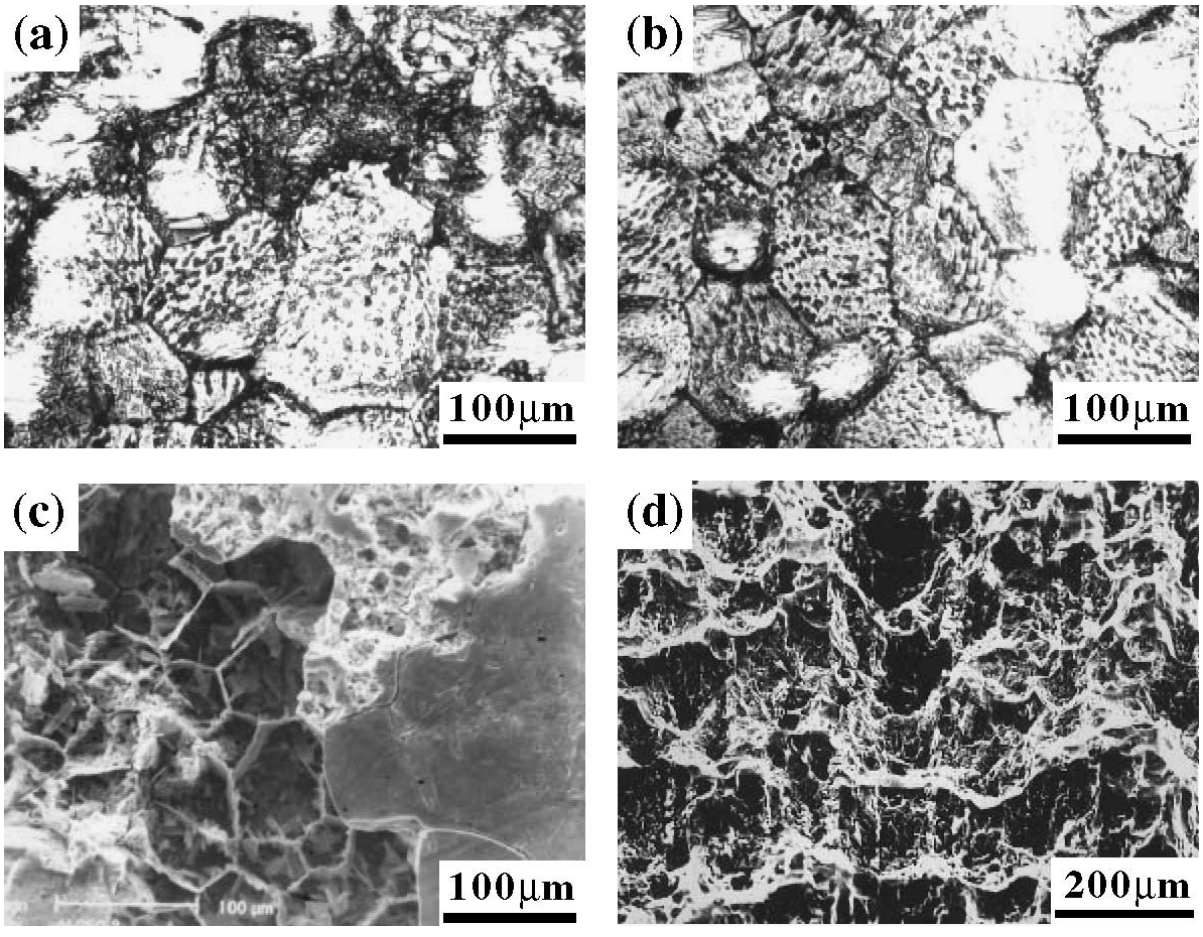

Figure 4 NAC morphology of the aluminized steel after: (a) 5 h, (b) 10 h, (c) 30 h, and (d) 500 h immersion at 250°C, TAN = 210 mgKOH/g.

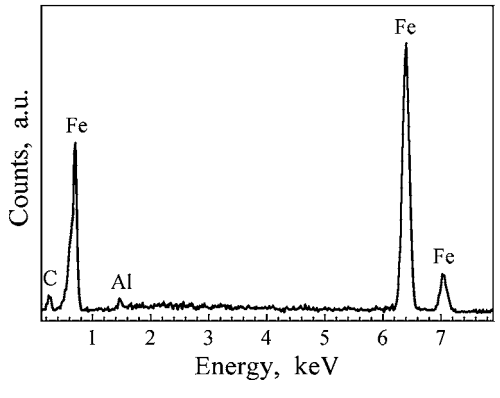

Figure 5 EDX surface analysis of the aluminized steel after 500 h immersion at 250°C, TAN = 210 mgKOH/g.

results of EDX analysis on the spallation areas (area A and B in Fig. 6d) and the remnants (area C in Fig. 6e). It was clear that with development of the spallation of the aluminized layer, the aluminum content in the surface-layer decreased gradually. At very high magnification, the surfaces of the corrosion steps were found to consist of fine and parallel grooves (Fig. 6f).

Fig. 8 shows typical NAC morphology after 100 h immersion at higher temperatures. At 250°C, more homogenous NAC took place on the surface of the carbon steel (Fig. 8a). There were many micro-cracks on the corroded surface when observed at high magnification (Fig. 8c). However, the aluminized steel suffered from quite inhomogenous NAC (Fig. 8b). Severe cracking and spallation took place in the aluminized layer. The skeleton-like remnants of the aluminized layer showed a very interesting morphology, which was similar to a bee's nest (Fig. 8d). EDX analysis revealed that these remnants were rich in aluminum, suggesting that they were similar to the remnants as shown in Fig. 6e. The exposed substrate under the nest, i.e., the carbon steel, was also subject to corrosion (indicated by the arrows in Fig. 8d). At 280°C, both the carbon steel and the aluminized steel suffered from severe NAC. A kind of corrosion pits or craters, whose diameter exceeded 100 μm, appeared on the surfaces of both materials (Figs 8e and f). A great number of micro-cracks were found inside these pits or craters.

3.2. NAEC tests in laboratory

Fig. 9 shows dependence of NAEC rate on the fluid velocity and the experimental temperature in relatively low-TAN (6.0 mgKOH/g) environment. It was clear that the NAEC rate increased with increasing fluid velocity and experimental temperature. For the carbon steel, the NAEC rate under the fast flow (U = 49 m/s) at 320°C was about 10 times as that under the slow flow ($U \cong$ 0 m/s) and was about 5 times as that at 220°C. The aluminized steel showed a much better NAEC resistance than the carbon steel in low-TAN environment. Under the same conditions of fluid velocity and temperature, the NAEC rate of the aluminized steel was about two orders of magnitude lower than that of the

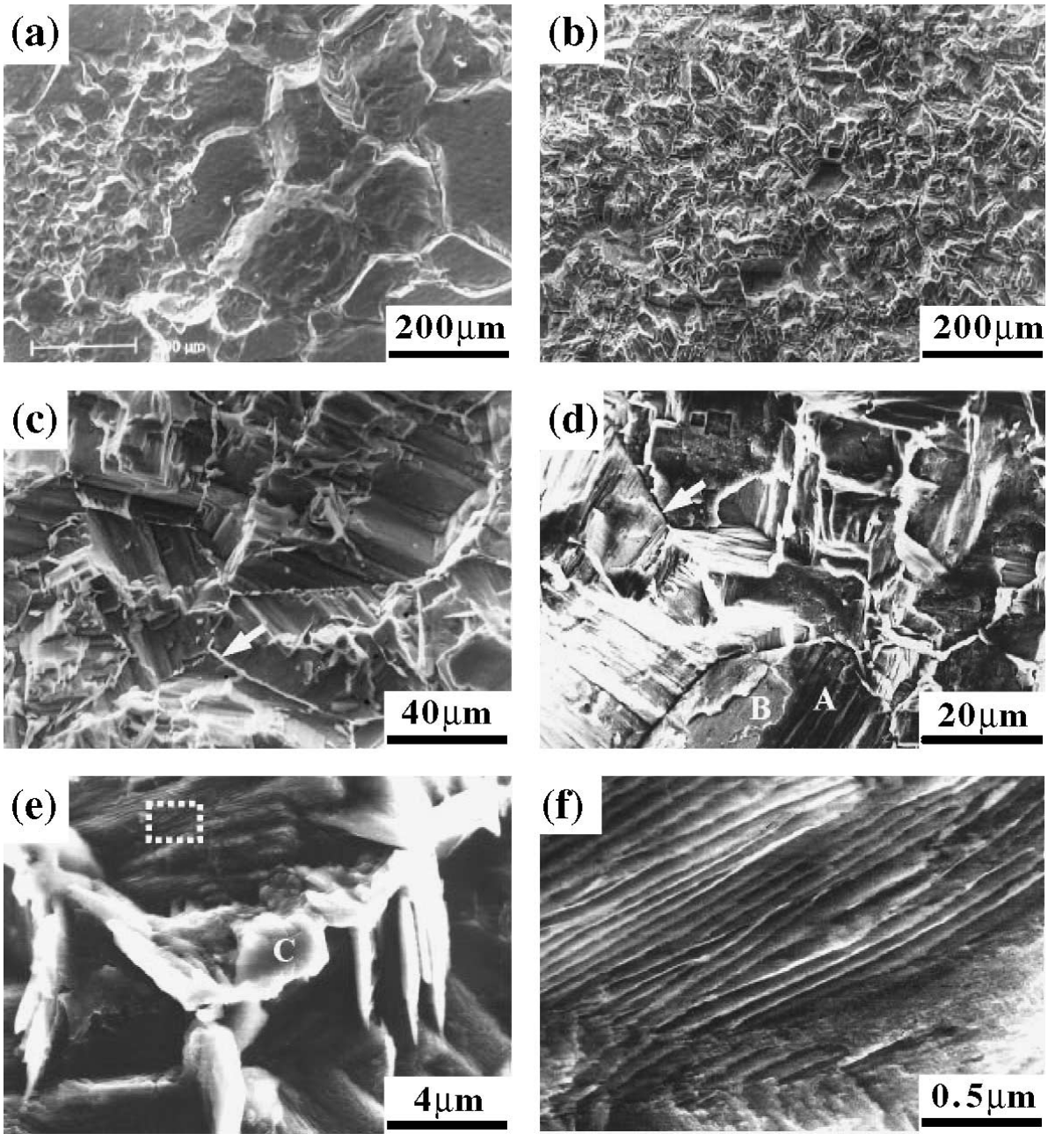

Figure 6 NAC morphology after 100 h immersion at 220°C, TAN = 210 mgKOH/g. (a) the carbon steel. (b) the aluminized carbon steel. (c) and (d) the high-magnification morphology of (b). (e) the morphology of the remains shown in (c). (f) the high-magnification morphology of the area marked in (e).

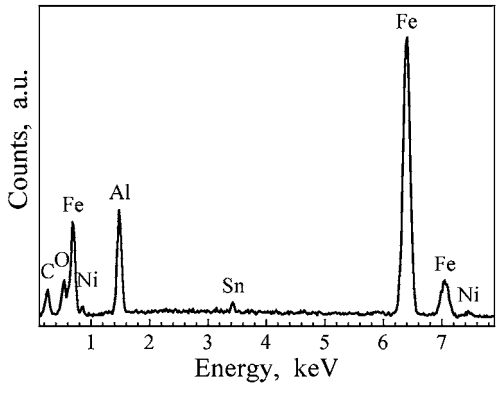

Figure 7 EDX surface analysis of the aluminized steel after 100 h immersion at 220°C, TAN = 210 mgKOH/g.

carbon steel. However, the detailed NAEC rate shown in the inset figure revealed that increasing the fluid velocity remarkably promoted the NAEC of the aluminized steel, especially at the higher temperatures.

Figs 10 and 11 show typical NAEC morphology of the carbon steel and the aluminized steel in low-TAN environment. Increasing the fluid velocity or the experimental temperature remarkably aggravated the NAEC. Under the slow flow ($U \cong 0$ m/s), some corrosion pits and cracks as well as residual metal scraps appeared on the surface of the steel carbon (Fig. 10a), while a slight attack (small cracks and pits) was observed along the grain boundaries for the aluminized steel (Fig. 11a). Under the fast flow ($U = 49$ m/s), distinct erosion-corrosion grooves were produced on

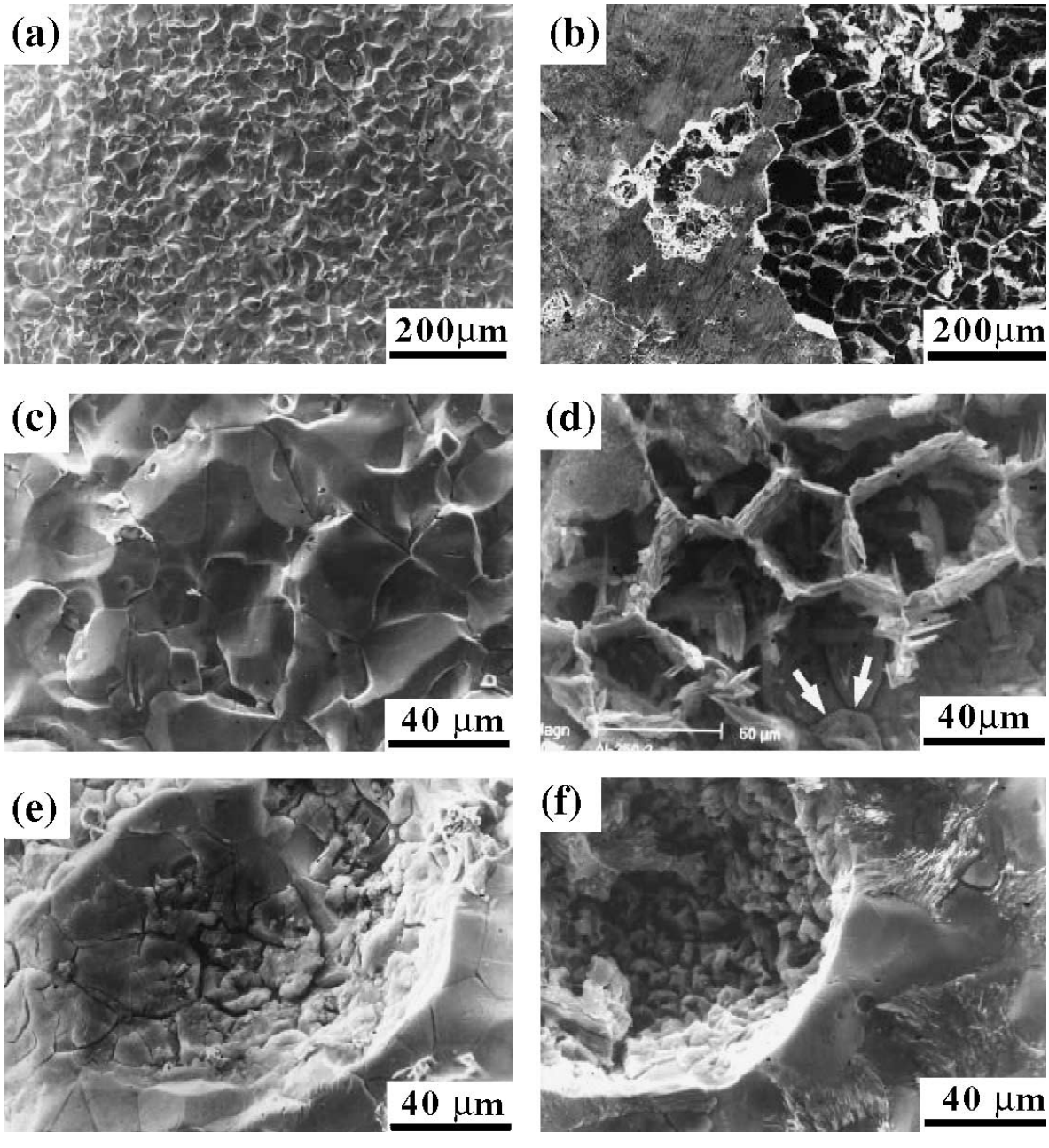

Figure 8 NAC morphology after 100 h immersion, TAN = 210 mgKOH/g. (a) the carbon steel, 250°C. (b) the aluminized steel, 250°C. (c) the high-magnification morphology of (a). (d) the high-magnification morphology of spallation area in (b). (e) the carbon steel, 280°C. (f) the aluminized carbon steel, 280°C.

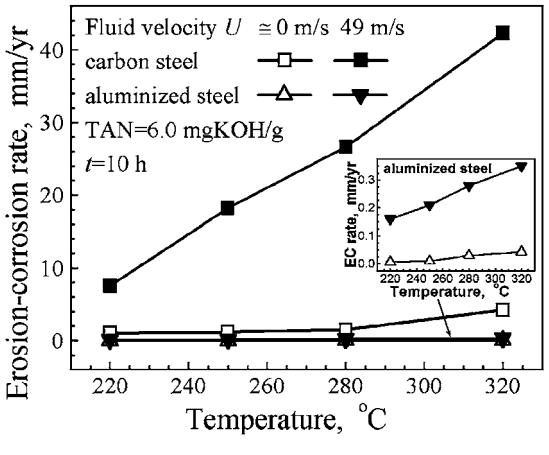

Figure 9 High-temperature NAEC rates of the carbon steel and the aluminized steel, the inset denotes detailed NAEC rate of the aluminized steel.

surface of the carbon steel (Fig. 10b). Moreover, the surface attack caused by the erosion-corrosion was aggravated observably with increasing experimental temperature (Fig. 10c and d). For the aluminized steel, the erosion-corrosion attack (cracks and pits) also became relatively serious under the fast flow (Fig. 11b). Increasing the experimental temperature caused the cankerous attack morphology appeared near the grain boundaries (Fig. 11c). After NAEC test at 320°C, the cankerous morphology became more frequent on surface of the aluminized steel and the spallation took place at local areas (Fig. 11d).

3.3. Erosion-corrosion tests in an oil refinery

Fig. 12 shows erosion-corrosion rate and thinning rate of the carbon steel and the aluminized steel after the

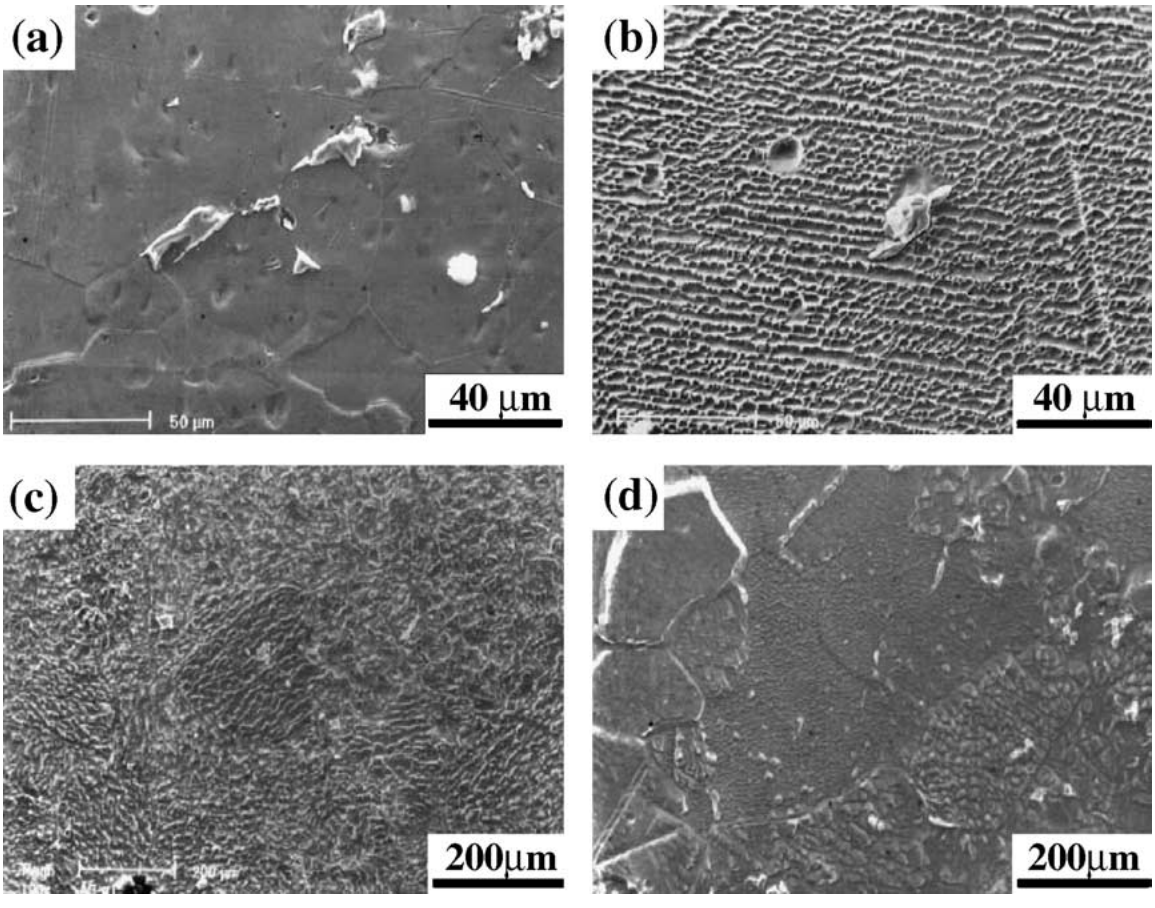

Figure 10 NAEC morphology of the carbon steel, TAN = 6.0 mgKOH/g. (a) $U \cong 0$ m/s, 250°C. (b) $U = 49$ m/s, 250°C. (c) $U = 49$ m/s, 280°C. (d) $U = 49$ m/s, 320°C.

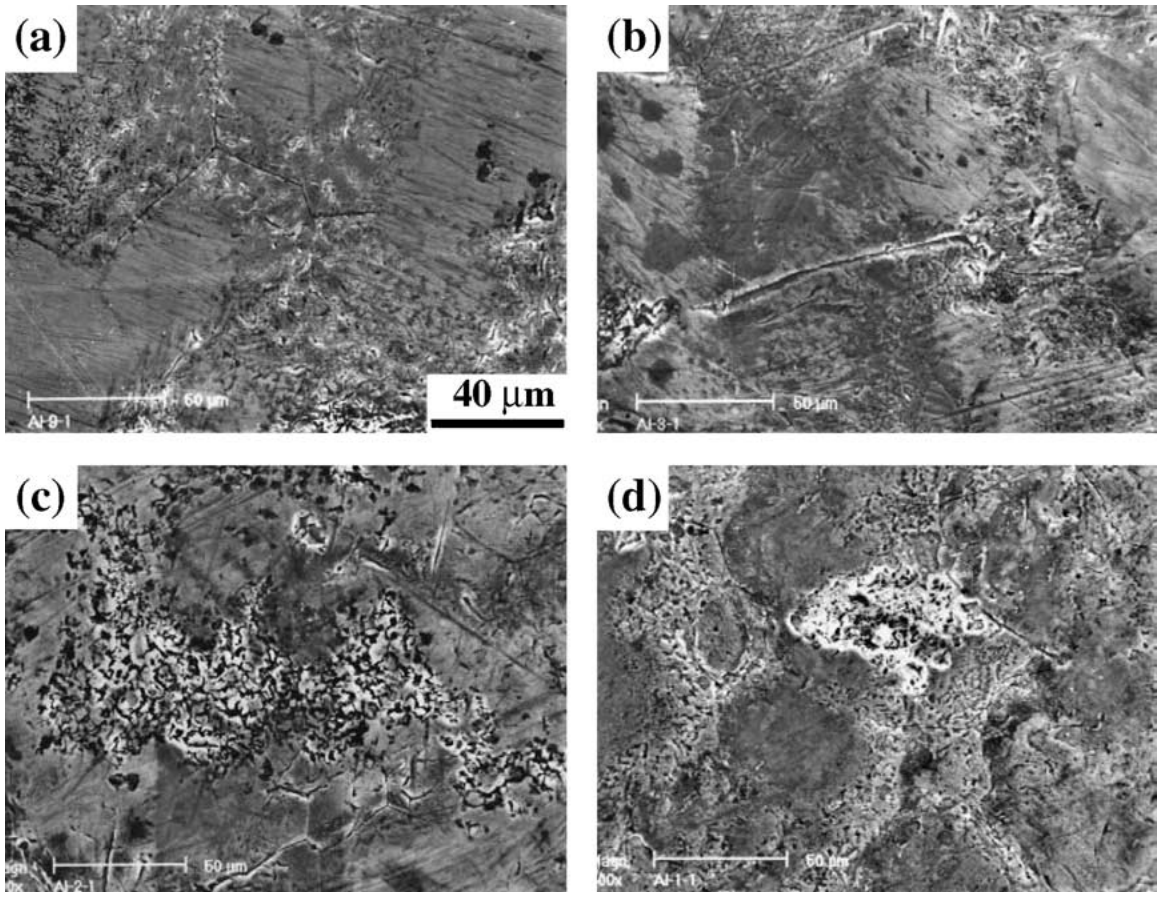

Figure 11 NAEC morphology of the aluminized steel, TAN = 6.0 mgKOH/g. (a) $U \cong 0$ m/s, 250°C. (b) $U = 49$ m/s, 250°C. (c) $U = 49$ m/s, 280°C. (d) $U = 49$ m/s, 320°C.

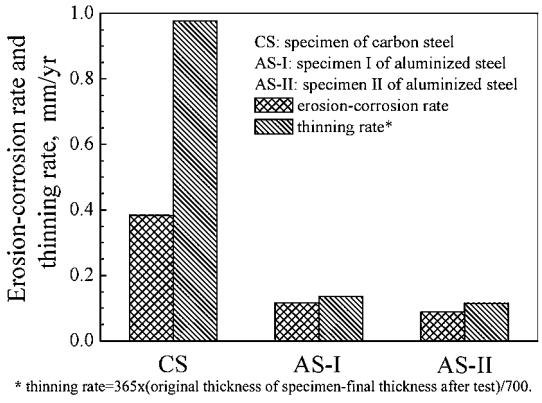

Figure 12 Erosion-corrosion rate and thinning rate of the carbon steel and the aluminized steel after the field test of 700 days in actual oil-refining environment.

field test of 700 days in an oil refinery. Similarly, the aluminized steel exhibited better erosion-corrosion resistance in actual oil-refining environment than the carbon steel. Moreover, the thinning rate of the aluminized steel was about one-seventh of that of the carbon steel.

Fig. 13 shows macro-morphology of the specimens after the field test of 700 days. The whole surface of the carbon-steel specimen had been attacked seriously and its bolt-holes were damaged seriously (Fig. 13a). The aluminized-steel specimens had deformed and their bolt-holes were also damaged moderately (Fig. 13b and c). However, it was clear that only partial surface of the aluminized-steel specimens had been attacked. When observed at high magnification, typical erosion-corrosion traces were found on surface of the carbon-steel specimen (Fig. 14a) as well as many erosion-corrosion cracks (Fig. 14b), while some spallation and cracks (Fig. 14c and d), whose morphology was similar to those observed previously in the NAEC tests in laboratory (Fig. 11), appeared on the attacked areas of the aluminized-steel specimens. EDX analysis revealed that the surface-layer of the aluminized steel was still rich in aluminum and minor sulfur trace was inspected on surfaces of both the carbon steel and the aluminized steel (Fig. 15).

4. Discussion

The typical NAC process is usually described as follows [1, 9],

$$2n\mathrm{RCOOH} + 2\mathrm{M} \rightarrow 2\mathrm{M(RCOO)}_n + n\mathrm{H}_2 \quad (2)$$

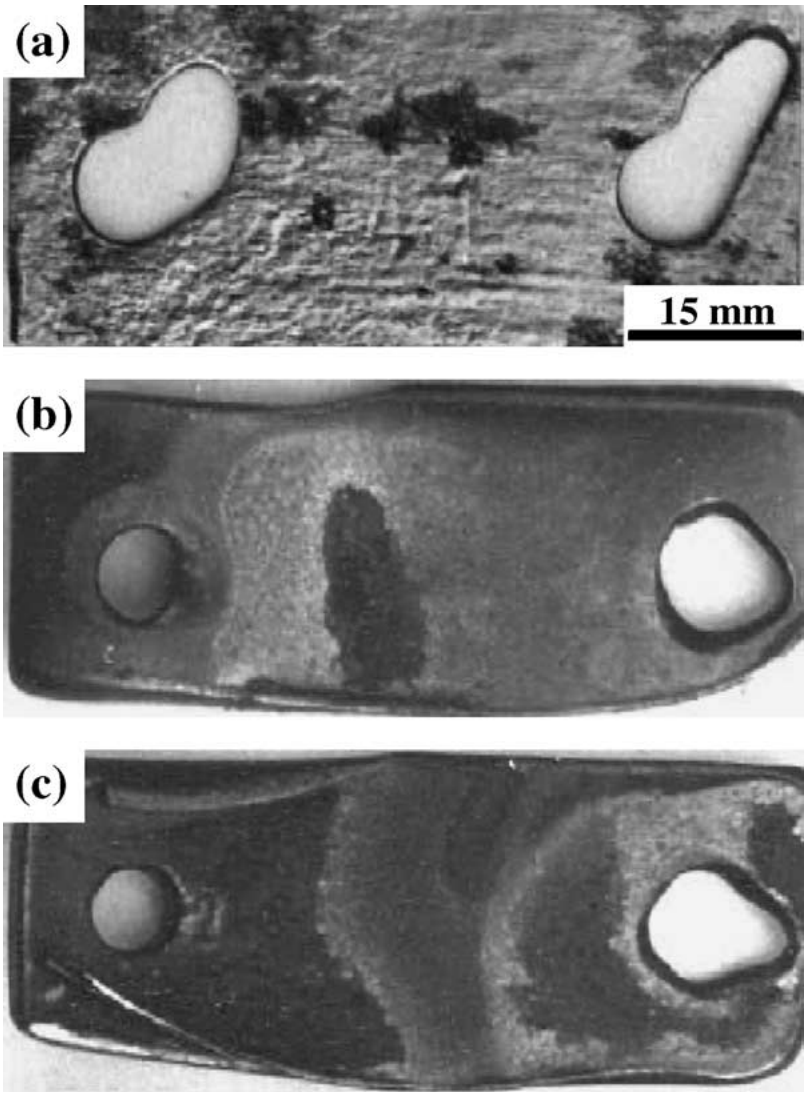

Figure 13 Morphology of the specimens after the field test of 700 days in an oil refinery. (a) specimen of the carbon steel. (b)(c) specimen I and II of the aluminized steel.

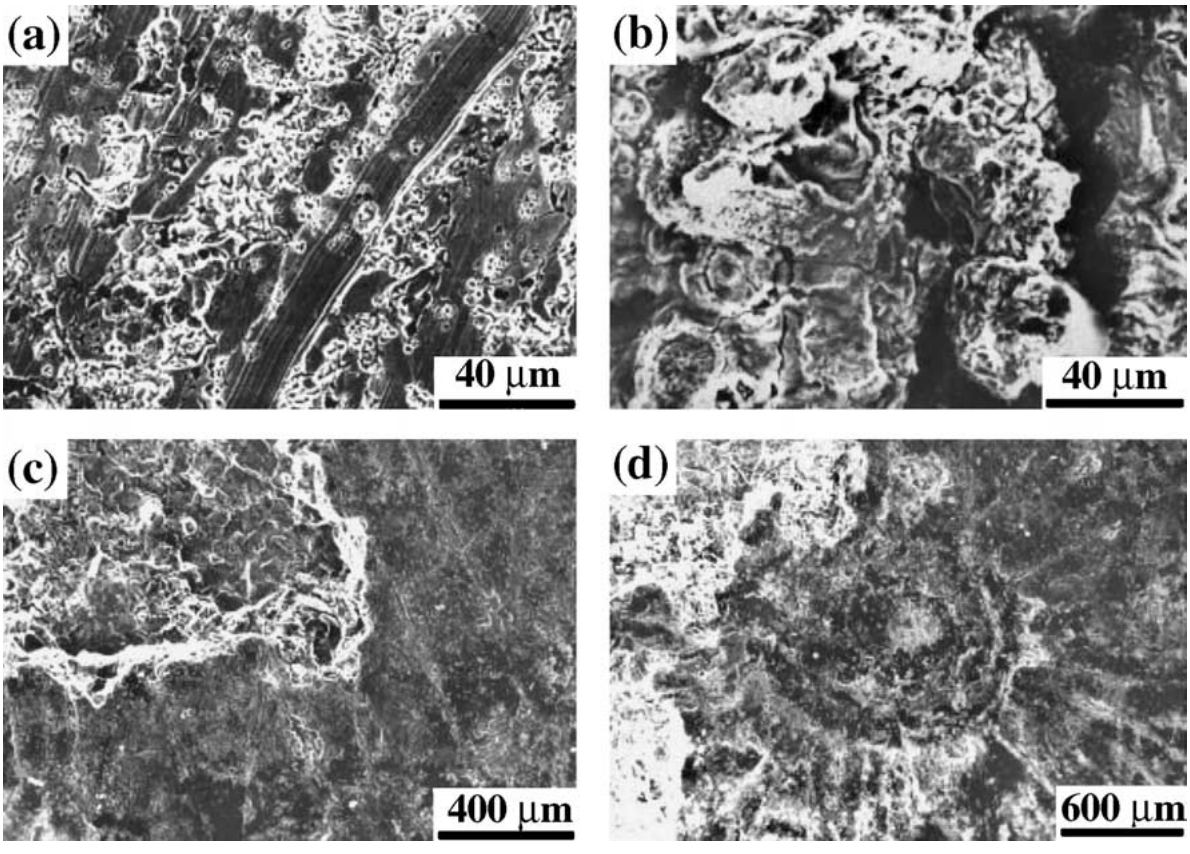

Figure 14 Erosion-corrosion morphology of the specimens after the field test of 700 days in an oil refinery. (a)(b) the carbon steel. (c)(d) the aluminized steel.

here R denotes the naphthenic radical, M denotes the susceptible metal, and $M(RCOO)_n$ denotes the corrosion product and is usually soluble in the naphthenic acids or oil media. The NAC process can be divided into four steps: (i) the transportation of the naphthenic acid molecules toward the metal surface; (ii) the absorption of the naphthenic acid molecules at the active sites on the metal surface; (iii) the reactions at the active sites on the metal surface; and (iv) the spallation or dissolution of corrosion products from the metal surface, each of which may significantly influence the NAC rate. Increasing the experimental temperature not only promotes the diffusion transportation of the naphthenic acid molecules toward the metal surface and the desorption or dissolution of the corrosion products from the metal surface, but also aggravates the reaction at surface active sites on the metal surface due to the endothermic nature of NAC reaction [4, 19]. Increasing the temperature, thus, aggravates the NAC, which is in accordance with presently NAC experimental results for both the carbon steel and the aluminized steel (Figs 3, 6 and 8).

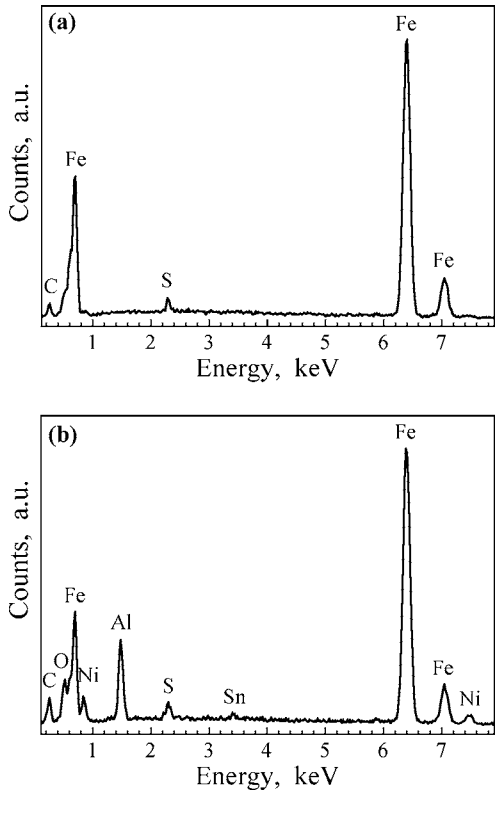

Figure 15 EDX surface analysis of the specimens after the field test of 700 days in an oil refinery. (a) the carbon steel. (b) the aluminized steel.

Here much attention should be paid on the NAC behavior of the aluminized steel in high-temperature and high-TAN (210 mgKOH/g) naphthenic acid media. It was found that the aluminized steel showed rapidly degraded NAC resistance in high-TAN environment with increasing immersion duration. As indicated by X-ray diffraction analysis (Fig. 1b) and EDX surface analysis (Fig. 7), the surface-layer of the aluminized steel was mainly composed of an inside layer of iron-aluminum ($Fe_{0.5}Al_{0.5}$ phase) and an outside film of aluminum-rich oxide (Al_2O_3). Undoubtedly, both the Al_2O_3 film and the iron-aluminum layer can play a role of barrier to prevent the direct contact between the susceptible metal (mainly Fe for present case) and the corrosive media if they firmly adhered to the matrix and kept integrated. Thus, the aluminized steel exhibited much lower NAC

rate at the early stage of immersion than the carbon steel that lacks of any protective film or layer (Fig. 2). However, it should be noted that the Al_2O_3 film is usually unstable in the acidic environments. Although the naphthenic acids are organically weak acids, following reaction may take place slowly in high-temperature and high-TAN environment with increasing immersion time.

$$Al_2O_3 + 6RCOOH \rightarrow 2Al(RCOO)_3 + 3H_2O \quad (3)$$

The Al_2O_3 film, thus, gradually degraded and was replaced by the soluble corrosion product $Al(RCOO)_3$. Then, the substrate, i.e., the iron-aluminum layer, was exposed directly to the corrosive media. Since this layer was relatively rich in Fe, it can provide many Fe-rich active sites for the surface reaction. The grain boundaries and some susceptible grains, therefore, were gradually subject to attack with increasing immersion time (Fig. 4a and b). Further development of the attack gave rise to the cracking or spallation of the iron-aluminum layer (Fig. 4c and d). Due to high microhardness and brittle nature, the iron-aluminum layer degraded in a step-like (Fig. 6c) or laminar spallation (Fig. 6d). Clearly, such kind of spallation tended to result in a rapid failure of the aluminized layer and thus make the matrix of carbon steel exposed directly to the corrosive media, especially at higher temperatures (Fig. 8b, d and f). This was believed to be a major reason that the NAC resistance of the aluminized steel degraded rapidly with increasing immersion time and became even worse than that of the carbon steel at the final stage of immersion (Fig. 2).

The naphthenic acids are actually composed of diversiform organic acids with different molecular weight (ranging from 200 to 300 averagely), ring structure and boiling point (ranging from 200°C to about 400°C) [2, 7]. Boiling, thus, may happen for some components with lower boiling point and bubbles may be produced in the media. The collapse of these bubbles on the metal surface may induce a sudden impact or damage, thus may result in the large craters as shown in Fig. 8e and f. In addition, the decomposition or evaporation of unstable components in the naphthenic acids will happen with increasing immersion time at high temperatures, which may weaken the corrosivity of the media and induce the variation in corrosion rate as shown in Fig. 2. Similar experimental results had been reported by Turnbull *et al.* [17].

In high-temperature and low-TAN (6.0 mgKOH/g) environment, the aluminized steel showed a much better resistance to the NAC and NAEC than the carbon steel, especially under the conditions of higher temperatures and fast flow ($U = 49$ m/s), as indicated by the NAEC rate and morphology (Figs 9–11). Since the lower the TAN of the corrosive media, the weaker the corrosivity appears. The reaction (3) is relatively difficult to process in low-TAN environment. The Al_2O_3 film and the iron-aluminum layer may work as relatively durable or effective barriers to prevent the contact between the corrosive media and the matrix of carbon steel. The aluminized steel, thus, exhibited a much better NAEC resistance. The influence of the fluid velocity on the NAC behavior has been discussed in detail in the previous work and were believed to be closely associated with the enhanced mass transfer and the accelerated surface reaction as well as the rapid spallation of corrosion products from the metal surface [20]. The excellent NAEC resistance of the aluminized steel in low-TAN environment may also be ascribed to its surface-layer. As stated previously, the microhardness of the aluminized layer was about three or four times as that of the carbon steel. Such high microhardness contributed a good resistance to the fluid erosion. Furthermore, the Al_2O_3 film and iron-aluminum layer kept relatively stable or durable in low-TAN corrosive media, and thus contributed a better endurance to the NAC. However, it should be noted from the NAEC morphology in Fig. 11 that surface-layer of the aluminized steel was also subject to attack to some extent, especially under the conditions of higher temperatures and fast flow, although it exhibited a much better NAEC resistance than the carbon steel.

In the present study, the aluminized steel also showed a good resistance to the erosion-corrosion in actual oil-refining environment (Figs 12–14). However, relatively serious attack also took place in the aluminized layer during the long-term test (Figs 13 and 14) although the TAN (0.9–1.2 mgKOH/g) in actual oil-refining environment is much lower than that used in the previous laboratory tests. This may be partly attributed to the influence of sulfur corrosion. The EDX analysis shown in Fig. 15 also suggested that sulfur play a role in erosion-corrosion process in actual oil-refining environment. According to the Table I, a certain amount (0.8–1.0%) of sulfur existed in the oil-refining environment studied presently. During the long-term test, the fluid erosion or other mechanical and chemical effects may remove the original Al_2O_3 film on surface of the aluminized steel, then following processes may take place on the substrate.

$$S + Fe \rightarrow FeS \quad (4)$$

$$2RCOOH + FeS \rightarrow Fe(RCOO)_2 + H_2S \quad (5)$$

$$Fe + H_2S \rightarrow FeS + H_2 \quad (6)$$

The FeS produced by reaction (4) or (6) tends to form a protective film on metal surface and offer some resistance to the NAC to some extent [1, 9]. However, the reaction (5) will cause the FeS film transform into the soluble $Fe(RCOO)_2$ and the active H_2S, which not only increased the attack tendency of the substrate, but also regenerates the sulfur source. Simultaneously, another reaction (7) may produce FeS precipitated in the corrosive media and regenerate the naphthenic acids.

$$Fe(COOH)_2 + H_2S \rightarrow FeS + 2RCOOH \quad (7)$$

The development and interaction of the above processes, thus, causes the NAC or the sulfur corrosion proceed continuously on the metal surface. In addition, the fluid erosion in the oil-refining environment may also accelerate the spallation of the FeS film. It

is believed that the combined effects of the fluid erosion and the NAC as well as the sulfur corrosion may aggravate the attack of the aluminized steel in actual oil-refining environment.

In view of the results mentioned above, due to its worse NAC resistance in high-TAN environment, the aluminized steel should be cautiously used as a component or replacement material at the locations where the acid concentration is relatively high in oil refineries. Typical locations or components are the underside of trays and downcomers where high concentration of acids condense from the vapor, the walls of the columns where are frequently subject to condensate rundown, bubble caps, stuff, demister pads and support grids in vacuum distillation towers, and so on. However, in view of its excellent NAC and NAEC resistance in low-TAN environment, the aluminized steel can used as a preferred material for the locations or components serving in the environments of low acid concentration and fast flow in oil refineries. Typical locations or components are the inner walls of furnace tubes or side cut piping or elbows, baffles, transfer lines, heat exchangers, pump impellers, and so on.

5. Conclusions

In high-TAN environment, the aluminized carbon steel exhibited a better resistance to the NAC only at the early stage of immersion than the carbon steel. The NAC resistance degraded rapidly with increasing immersion time, and became even worse than that of the carbon steel at the final stage of immersion, accompanying a step-like or lamellar spallation in the aluminized layer. In low-TAN environment, the aluminized carbon steel exhibited a much better resistance to both the NAC and NAEC in comparison with the carbon steel.

The rapidly degraded NAC resistance of the aluminized carbon steel with increasing immersion duration may be attributed to the instability of its surface-layer (Al_2O_3 film and iron-aluminum alloy layer) in high-TAN environment. The excellent NAC and NAEC resistance of the aluminized carbon steel in low-TAN environment may be due to the higher microhardness and the relatively durable or effective barrier effects of its surface-layer.

The aluminized carbon steel also exhibited a good resistance to the erosion-corrosion in actual oil-refining environment although relatively serious erosion-corrosion attack also took place in the aluminized layer. The combined effects of the fluid erosion and the NAC as well as the sulfur corrosion may aggravate the attack of the aluminized carbon steel in actual oil-refining environment.

In view of the presently experimental results, it was suggested that the aluminized carbon steel should be cautiously used as a component or replacement material at the locations where the acid concentration is relatively high in oil refineries, while it can be used as a preferred material for the locations or components serving in the environments of low acid concentration and fast flow.

Acknowledgements

This work was supported by funds from the Science and Technology Foundation of Liaoning Province (001012) and the Sinopec Technology Company. We are grateful for their supports.

References

1. E. SLAVCHEVA, B. SHONE and A. TURNBULL, *Br. Corros. J.* **34** (1999) 125.
2. W. A. DERUNGS, *Corrosion* **12** (1956) 617t.
3. A. J. BREEN, *Br. Corros. J.* **9** (1974) 197.
4. J. GUTZEIT, *Mater. Perform.* **16** (1977) 24.
5. B. F. ERNESTO and H. BRIAN, *Corrosion'83* (1983), Paper No. 99.
6. G. L. SCATTERGOOD, R. C. STRONG and W. A. LINDALEY, *Corrosion'87* (1987), Paper No. 197.
7. R. L. PIEHL, *Mater. Perform.* **27** (1988) 37.
8. D. C. AGARWAL, U. BRILL and U. HEUBNER, *Corrosion' 92* (1992), Paper No. 451.
9. E. B. KIBALA, H. L. CRAIG, G. L. RUSK, K. V. BLANCHARD, T. J. ROSE, B. L. UEHLEIN, R. C. QUINTER and M. A. SUMMERS, *Mater. Perform.* **32** (1993) 50.
10. A. JAYARAMAN and R. C. SAXENA, *Corros. Prevent. Control* **42** (1995) 123.
11. H. L. CRAIG, *Corrosion'95* (1995), Paper No. 333.
12. M. J. ZETLMEISL, *Corrosion'95* (1995), Paper No. 334.
13. *Idem., Corrosion'96* (1996), Paper No. 218.
14. H. L. CRAIG, *Corrosion'96* (1996), Paper No. 603.
15. B. E. HOPKIASON and S. A. LAGOVEN, *Corrosion'97* (1997), Paper No. 502.
16. A. TURNBULL, E. SLAVCHEVA and B. SHONE, *Corrosion* **54** (1998) 922.
17. R. D. KANE and M. S. CAYARD, *Mater. Perform.* **38** (1999) 48.
18. S. TEBBAL, *Corrosion'99* (1999), Paper No. 380.
19. Y. M. GAO, J. J. CHENG, G. YU, H. Y. YANG, D. Z. CAO and Y. J. ZHU, *Corros. Sci. Protect. Technol.* (*in Chinese*) **12** (2000) 27.
20. X. Q. WU, H. M. JING, Y. G. ZHENG, Z. M. YAO and W. KE, *Mater. Corros.* **53** (2002) 833.

Received 4 February
and accepted 24 September 2003